ResearchGate

See discussions, stats, and author profiles for this publication at: https://www.researchgate.net/publication/338244744

On-road gaseous and particulate emissions from GDI vehicles with and without gasoline particulate filters (GPFs) using portable emissions measurement systems (PEMS)

Article *in* Science of The Total Environment · December 2019

DOI: 10.1016/j.scitotenv.2019.136366

CITATIONS
0

READS
120

9 authors, including:

Cavan McCaffery
University of California, Riverside
1 PUBLICATION **0** CITATIONS
SEE PROFILE

Hanwei Zhu
Peking University
8 PUBLICATIONS **18** CITATIONS
SEE PROFILE

Li Chengguo
University of California, Riverside
15 PUBLICATIONS **462** CITATIONS
SEE PROFILE

Thomas D. Durbin
University of California, Riverside
150 PUBLICATIONS **2,591** CITATIONS
SEE PROFILE

Some of the authors of this publication are also working on these related projects:

Emissions from Plug-in Hybrid Electric Vehicle (PHEV) During Real World Driving Under Various Weather Conditions View project

DownToTen - Measuring Automotive Exhaust Particles Down To 10 Nanometers View project

All content following this page was uploaded by Li Chengguo on 15 January 2020.

The user has requested enhancement of the downloaded file.

Science of the Total Environment 710 (2020) 136366

Contents lists available at ScienceDirect

Science of the Total Environment

journal homepage: www.elsevier.com/locate/scitotenv

On-road gaseous and particulate emissions from GDI vehicles with and without gasoline particulate filters (GPFs) using portable emissions measurement systems (PEMS)

Cavan McCaffery [a,c], Hanwei Zhu [a,b], Chengguo Li [a], Thomas D. Durbin [a,b], Kent C. Johnson [a,b], Heejung Jung [a,c], Rasto Brezny [d], Michael Geller [d], Georgios Karavalakis [a,b,*]

[a] University of California, Bourns College of Engineering, Center for Environmental Research and Technology (CE-CERT), 1084 Columbia Avenue, Riverside, CA 92507, USA
[b] Department of Chemical and Environmental Engineering, Bourns College of Engineering, University of California, Riverside, CA 92521, USA
[c] Department of Mechanical Engineering, Bourns College of Engineering, University of California, Riverside, CA 92521, USA
[d] Manufacturers of Emission Controls Association, 2200 Wilson Boulevard, Suite 310, Arlington, VA 22201, USA

HIGHLIGHTS

- Catalyzed GPFs showed significant reductions in real-world PM emissions.
- Urban and high-altitude driving showed elevated PM emissions.
- Highest particle number concentrations were seen for low speeds and positive accelerations.
- Real-world NOx emissions showed reductions with the catalyzed GPFs.

GRAPHICAL ABSTRACT

ARTICLE INFO

Article history:
Received 16 October 2019
Received in revised form 14 December 2019
Accepted 25 December 2019
Available online 30 December 2019

Editor: Karl Ropkins

Keywords:
PEMS
Gasoline direct injection
Real-world emissions
PM emissions
NOx emissions

ABSTRACT

This study assessed the on-road gaseous and particulate emissions from three current technology gasoline direct injection (GDI) vehicles using portable emissions measurement systems (PEMS). Two vehicles were also retrofitted with catalyzed gasoline particulate filters (GPFs). All vehicles were exercised over four routes with different topological and environmental characteristics, representing urban, rural, highway, and high-altitude driving conditions. The results showed strong reductions in particulate mass (PM), soot mass, and particle number emissions with the use of GPFs. Particle emissions were found to be highest during urban and high-altitude driving compared to highway driving. The reduction efficiency of the GPFs ranged from 44% to 99% for overall soot mass emissions. Similar efficiencies were found for particle number and PM mass emissions. In most cases, nitrogen oxide (NOx) emissions showed improvements with the catalyzed GPFs in the underfloor position with the additional catalytic volume. No significant differences were seen in carbon dioxide (CO_2) and carbon monoxide (CO) emissions with the vehicles retrofitted with GPFs.

© 2018 Elsevier B.V. All rights reserved.

* Corresponding author at: University of California, Bourns College of Engineering, Center for Environmental Research and Technology (CE-CERT), 1084 Columbia Avenue, Riverside, CA 92507, USA.
E-mail address: gkaraval@cert.ucr.edu (G. Karavalakis).

https://doi.org/10.1016/j.scitotenv.2019.136366
0048-9697/© 2018 Elsevier B.V. All rights reserved.

1. Introduction

Road transport is a major source of nitrogen oxides (NOx) and particulate matter (PM), impacting air quality throughout the world. Elevated concentrations of mobile source emissions are responsible for adverse health impacts, including respiratory and cardiovascular diseases, or even premature mortality (Kampa and Castanas, 2008; Bates et al., 2015). Mobile source emissions have been significantly changed over the years as a result of stricter vehicle emission standards and efforts to reduce greenhouse gas (GHG) emissions. In the United States (US), Corporate Average Fuel Economy (CAFE) standards are pushing automotive manufacturers to meet fuel economy levels for passenger cars. Similarly, carbon dioxide (CO_2) emissions from newly registered cars in the European Union (EU) must decrease to about 95 g per kilometer by 2021.

The share of gasoline direct injection (GDI) engines has grown rapidly in both the US and the EU. GDI technology enables both an increase in specific power and a better fuel economy (with simultaneous reduction in CO_2 emissions), compared to traditional port fuel injection (PFI) engines (Alkidas, 2007). However, GDI engines are known to produce higher PM mass, black carbon, and particle number emissions than PFI engines and modern technology diesel engines equipped with diesel particulate filters (DPFs) (Karavalakis et al., 2015; Saliba et al., 2017; Zinola et al., 2016). PM formation in GDI engines is due to partially evaporated liquid fuel leading to fuel rich regions in the combustion chamber that promote the generation of PM (Karlsson and Heywood, 2001; Piock et al., 2011). Studies have shown that most GDI PM emissions are formed during the cold-start phase and during highly transient operations (Chen et al., 2017; Koczak et al., 2016). The dynamic market penetration of GDI engines along with their elevated PM emissions create a growing public health concern in terms of PM exposures in urban areas.

Concerns about the real-world performance of vehicles and the lack of real-world operation represented of chassis dynamometer tests are now being addressed with test protocols capable of characterizing real-world vehicle emissions. Portable emissions measurement systems (PEMS) have been widely used to measure vehicle gaseous and particulate emissions under real-world conditions (Weiss et al., 2011; Gallus et al., 2016; Kwon et al., 2017; Yang et al., 2018a). PEMS have been proved to be an important tool for emission inventories because they enable testing under a wide variety of driving conditions, including road gradients, altitude and environmental conditions variations, and strong accelerations (Zhang et al., 2019; Bishop et al., 2019; O'Driscoll et al., 2018). In the US, PEMS measurements are required for in-use compliance testing of heavy-duty diesel vehicles, while the EU has implemented PEMS-based type-approval testing for light-duty vehicles starting from the Euro 6 standards. Overall, previous work has shown that there are substantial differences in emissions measured on-road using PEMS compared to laboratory testing (May et al., 2014; Chossière et al., 2018; Fontaras et al., 2017; Andersson et al., 2014). A number of studies have been conducted on different types of vehicles using PEMS, including heavy-duty trucks (Mendoza-Villafuerte et al., 2017; Johnson et al., 2009) and light-duty diesel and gasoline cars (Valverde et al., 2019; Khan and Frey, 2018), and off-road equipment (Cao et al., 2016; Cao et al., 2018). Gallus et al. (2017) found CO_2 and nitrogen oxides (NOx) emissions were strongly correlated with driving parameters, showing increases with road grade. Wang et al. (2018) reported increases in carbon monoxide (CO), NOx, and particle number emissions at elevated altitude. Other PEMS studies have shown that real-world NOx and particulate emissions are affected by fuel type, after-treatment control, and engine power (Quiros et al., 2016; Huang et al., 2013; Demuynck et al., 2017).

The introduction of more challenging test procedures, such as real-driving emissions (RDE) for type approval in the EU, as well as stricter emission standards, such as the California LEV III PM mass limit of 1 mg/mile beginning in 2025 and the Euro 6a particle number limit of 6×10^{11} particles/km, make the reductions in target pollutants more difficult to be met with engine improvements alone. While stricter solid particle number regulations in the EU may have led to the introduction of gasoline particulate filters (GPFs) in the passenger car fleet there, at the time it is not expected that GPFs will be widely adopted in the US. Several studies have reported that the use of GPFs resulted in dramatic reductions in PM mass, number, and black carbon emissions from GDI vehicles (Yang et al., 2018b; Araji and Stokes, 2019). A recent study even showed that the use of catalyzed GPFs can reduce secondary organic aerosol formation (Roth et al., 2019). In addition, studies have shown reductions in particulate emissions and improved conversion efficiencies for CO and NOx emissions with the use of catalyzed GPFs under real-world conditions with minimal impact on CO_2 emissions (Schoenhaber et al., 2017; Yoshioka et al., 2019). Demuynck et al. (2017) investigated the deployment of GPFs on GDI vehicles using PEMS and found significant reductions in particle number emissions under RDE conditions. A similar study also showed reductions in particle number emissions with the use of GPFs, without any detectable increase in CO_2 emissions (Ogata et al., 2017).

The primary objective of this study was to improve our understanding of the particulate emissions from three current technology GDI light-duty vehicles under different driving conditions mimicking urban, rural, and highway driving patterns, and included changes in altitude, road grade, and environmental conditions. Emissions testing were conducted on two vehicles in the stock configuration as well as after replacing the OEM underfloor three-way catalyst (TWC) with a catalyzed GPF. The catalyst formulation on the GPF was typical of an underfloor catalyst on vehicles of the same class, however, no attempt was made to exactly match the GPF catalyst formulation with that on the stock underfloor converter. Furthermore, the mileage accumulated on the GPF was not matched with the mileage of the TWC that it replaced. Therefore, the gaseous emissions are provided as observations for the purpose of relative comparison and are not intended to draw absolute conclusions. The results of this study will be useful in understanding real-world emissions from GDI vehicles and their contribution to air pollution in the Los Angeles Basin and other urban areas.

2. Experimental

2.1. Vehicles and GPFs

Three 2017 and 2018 model year GDI vehicles, referred to as GDI1, GDI2, and GDI3, were tested on-road for gaseous and particulate emissions. Detailed descriptions of the test vehicles are shown in Table 1. GDI1 and GDI3 were equipped with naturally aspirated engines and wall-guided fuel injection systems, whereas GDI2 was equipped with a turbocharged engine and a centrally-mounted fuel injection system. All vehicles were operated with overall stoichiometric air-fuel ratios and certified to meet the Federal Tier 3 emission standards. Testing on all vehicles was performed on typical California E10 fuel.

For GDI1 and GDI2, testing was also conducted with a catalyzed GPF installed in the place of the underfloor TWC. The original close-coupled catalysts were retained in their stock location. The GPFs were sized based on the engine displacement of each vehicle and they were catalyzed with precious metal loadings typical of underfloor catalysts at the same certification levels of the two vehicles. Both GPFs were 4.66 in. in diameter and 4.5 in. in length, with an 8-mil cell wall thickness and a cell density of 300 cells per square inch (cpsi). More details on the GPFs are provided in Yang et al. (2018b). Briefly, both GPFs followed a de-greening process, which included on-road highway driving of the vehicles for about 500 miles. Both GPFs were wall-flow type. Considering the low level of PM emissions for GDI vehicles compared to heavy-duty diesel vehicles, it is assumed the GPF fill state may not have changed significantly during the test period.

Table 1
Technical specifications of the test vehicles.

	GDI1	GDI2	GDI3
Vehicle model year	2017	2017	2018
Cylinder number	4, inline	4, inline	V6
Displacement	2.0 L	1.5 L	3.6 L
Horsepower	155 at 6000 rpm	181 at 6300 rpm	305 at 6800 rpm
Torque	150 lb-ft at 4000 rpm	185 lb-ft at 4320 rpm	264 lb-ft at 5200 rpm
Compression ratio	13.0:1	10.0:1	11.5:1
Air Intake	Naturally aspirated	Turbocharged	Naturally aspirated
Fuel delivery	Wall-guided	Centrally-mounted	Wall-guided
Emission standards	USEPA: T3B30, CA SULEV 30 PZEV	USEPA: T3B30, CA SULEV 30 PZEV	USEPA: T3 LDV, CA SULEV 30

2.2. PEMS installation

The PEMS units employed in this work to measure gaseous and particulate emissions were compliant with federal test methods (CFR 1065) for on-road testing and installed following manufacturers recommendations. PEMS installation included the use of a generator for power, backup lithium batteries, and a power inverter. The PEMS units were placed inside the vehicles (backseats and trunk), while the generator was attached to a hitch at the back of each vehicle. Prior the on-road testing, a calibration procedure including leak checks and zero-span calibration was performed.

For GDI1, the AVL 493 M.O.V.E gas PEMS and the AVL 494 PM PEMS systems were used. The AVL 493 PEMS system measures NOx (NO and NO_2) using non-dispersive ultraviolet radiation (NDUV), CO and CO_2 using non-dispersive infrared radiation (NDIR), and THC using flame ionization detection (FID). The AVL 494 PM PEMS system includes a dilution sampling system and a real-time AVL 483 micro soot sensor (MSS), in conjunction with AVL's integrated gravimetric PM filter module. For GDI2 and GDI3, the Sensors Semtech-DS unit was employed for the measurement of NOx, CO, CO_2, and THC emissions and the AVL 494 PM PEMS system. Solid particle number emissions according to the European Particle Measurement Programme (PMP) were measured for GDI1 and GDI3 vehicles with the use of AVL's M.O.V.E PN PEMS iS, which uses diffusion charger technology. For GDI2, particle number emissions were measured with the NTK NCEM mini-PEMS unit. This system measures PM mass and particle number emissions using a sensor based on the Pegassor PPS-M technology, where particles are charged in a corona discharge, such that the total measured charge is proportional to the particle active surface area. The NTK NCEM measures total particle number including solid and volatile particles and does not comply with the PMP protocol that excludes volatile particles and solid particles <23 nm. More details on the NTK NCEM systems are given elsewhere (Yang et al., 2018a). GDI1 and GDI 3 used a Sensors Inc. 2.5-in. exhaust flow meter (EFM) system, whereas GDI2 used a Sensors Inc. 2-in. EFM to provide integrated mass emissions as well as second by second emissions data. The EFM systems were equipped with an averaging pitot tube and thermocouples to obtain the exhaust mass flow. Both systems were designed to have wide dynamic range to measure exhaust flows so that the vehicle exhaust can be measured over the full range. Both EFM systems were calibrated following procedures according to CFR40 Part 1065.307. Table SM1 (Supplementary Material, SM) summarizes vehicles, PEMS units used, and test routes.

2.3. Test routes

On-road testing was performed in triplicate for each vehicle on four routes with different topological and environmental characteristics (Fig. SM1-Fig. SM4, SM). The test routes were designed to represent urban, rural, and highway driving conditions and included changes in altitude and ambient climatic conditions. The first route, referred to as Downtown Los Angeles (LA), primarily consisted of urban driving in the downtown area of LA and had a total distance of 16 miles. This route was characterized by dense traffic, frequent start and stop conditions, and an average speed of 15.7 miles/h. The route was created from the same route used to develop the LA Route Four (LA4) as part of the original certification Federal Test Procedure (FTP). The second route, referred to as Highway, started from LA and headed east to Ontario. This route utilized Interstate-10 (I-10), which is one of Southern California's major freeways. This route mainly consisted of high-speed driving with some congestion coming out of LA. The route covered a distance of 43 miles and had an average speed of 48.3 miles/h. The third route, referred to as Mountain (Mt) Baldy, consisted of mountainous roads with uphill/downhill driving, steep road grades, and medium to higher speeds during operation. The route started and ended at sea level, while on elevation change of 1524 m to the top of the mountain. It also consisted of some urban/rural driving on the historic route 66 and highway driving at high speeds. The average speed for this 44.2-mile route was 25.1 miles/h. The last and fourth route, referred to as Downtown San Diego (SD), started and ended in downtown San Diego on sea level roads near the harbor. This 13.1-mile route consisted of mainly urban driving with some highway portions in the Interstate-5. It was also characterized by high humidity with moderate temperatures. The total elevation change for the route was around 60 m. The Downtown LA and Downtown SD routes were similar in that both consisted of largely urban driving with some highway driving, but the Downtown SD route had more elevation changes and a lower average speed of 13.1 miles/h.

All PEMS emissions tests were conducted in the same sequence. For a single testing day, tests started with the Downtown LA route, followed by the Highway route, and ended with the Mt. Baldy route. The Downtown SD route was tested on a separate day. Testing on all routes was performed when the engine and TWC were fully warmed up. Cold-start emissions were obtained at the beginning of each test day prior to the vehicle's arrival on the testing site.

3. Results and discussion

3.1. Particulate emissions

Fig. 1(a–b) show the soot mass or black carbon emissions and gravimetric PM mass, respectively. For all vehicles on all test routes, PM mass emissions were below the Tier 3 PM mass standard of 3 mg/mile. Consistent with previous studies, the use of catalyzed GPFs resulted in important reductions in PM mass and black carbon emissions (Yang et al., 2018b; Chan et al., 2014). The decreases in PM emissions with the GPFs ranged from 12%–49% for GDI1 and 60%–96% for GDI2. Similar filtration efficiencies were also observed for the soot mass emissions, ranged from 44%–66% for GDI1 and 93%–99% for GDI2. Our results showed some higher GPF filtration efficiencies for the urban test routes compared to the Highway route, which agrees with the results of Yoshioka et al. (2019). The quasi steady-state operation of the engine over the Highway route may have led to more fuel cut-off and oxygen-rich phases, which prevented the formation of a soot layer in the filter channels due to passive regeneration. This was most likely

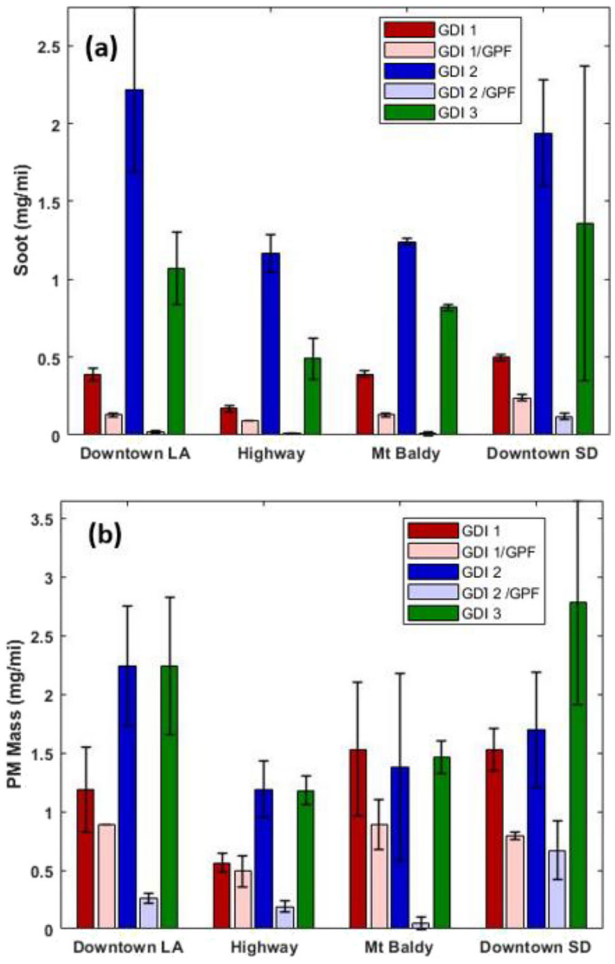

Fig. 1. (a–b): Soot mass and gravimetric PM mass emissions for the test vehicles over the different routes.

the reason for the lower filtration efficiency of GDI1 due to the lower engine-out PM levels compared to GDI2.

The higher compression ratio Atkinson engine equipped GDI1 generally showed lower PM mass and soot mass emissions over all test routes compared to GDI2 and GDI3, with the exception of the Mt. Baldy route where the differences in PM mass emissions were indistinguishable between the three vehicles. Yang et al. (2018b) attributed these phenomena to the earlier fuel injection and the subsequent formation of a homogeneous air-fuel mixture because of more time for mixture preparation. In addition, the higher in-cylinder temperature may have led to better oxidation of soot particles and hydrocarbon gases inside the combustion chamber, which will result in lower engine-out PM mass and soot.

Overall, PM mass and soot emission rates were higher for the urban routes (i.e., Downtown LA and Downtown SD) compared to the Highway route. Both urban routes included increased transient and aggressive driving with frequent stop-and-go events, which lead to greater particulate emissions. The large number of stop-and-go events for the urban test routes compared to highway driving caused increased PM mass and soot mass emissions per mile. Compared to the Highway route, Mt. Baldy showed elevated PM mass and soot emission rates. A recent study suggested that the lower oxygen concentration at higher altitudes may help to enhance the formation of PM emissions (Wang et al., 2018). For the Mt. Baldy route, uphill driving showed higher soot mass emissions and lower PM and soot percentage reductions for the GPF retrofitted vehicles compared to downhill driving (Table SM2, SM). The positive road grade for uphill driving is linked to higher load and acceleration events on the engine, which caused higher soot mass emissions and generally lower PM mass and soot percentage reductions for the GPFs. It should be noted that the Downtown SD route generally showed trends of higher PM emissions than the downtown LA route. The climatic conditions between these two routes likely influenced PM emissions, with generally lower ambient temperatures and high humidity in the San Diego area due to the very close proximity to the sea. This contributed to more PM formation by the combination of PM and moisture coming from the ambient air and also generated by exhaust gas condensation (Kwon et al., 2017).

Soot mass and particle number emissions were affected by vehicle speed and load for every test route, as shown in Table SM3-Table SM6 (SM). For the Downtown LA, Downtown SD, and Highway routes, the highest soot mass and particle number emissions were seen for the speed bins between 0 and 10 miles/h and 10–20 miles/h, and positive acceleration conditions from a stop ($a > 0$ m/s^2). These findings are graphically depicted in Fig. 2(a–d) for the solid particle number emissions for GDI1, while Fig. SM5 (SM) shows the soot mass emissions for GDI1. Urban driving includes a large amount of idling, congestion, and start/stop traffic conditions. This is an important finding from a PM exposure perspective, since these driving conditions usually occur in densely populated urban centers. Under deceleration conditions ($a < 0$ m/s^2) or relatively high speeds, soot mass and particle number emissions were lower, suggesting that free-flow driving at higher speeds in urban centers will not contribute to high concentrations of particulate emissions. For the Highway route, soot mass and particle number emissions showed elevated concentrations at low and intermediate speed bins and during acceleration events, suggesting that the bulk of these emissions were spikes formed during acceleration events as opposed to steady-state high speed driving. For the Mt. Baldy route, the intermediate speed bins (30–40 miles/h and 40–50 miles/h) and high accelerations produced higher soot mass and particle number emissions. GDI1 showed a 65% reduction in soot mass emissions with the GPF for the 0–10 miles/h speed bin that gradually decreased towards higher speed bins, with the lowest soot mass reduction with the GPF of 36% for the 50–60 miles/h speed bin. GDI2 showed strong soot mass reductions with the GPF (>99%) for all speed bins. Overall, soot mass and particle number emissions increased with engine loading for all test routes and vehicles. The soot mass reductions for both GPF-retrofitted vehicles tended to be higher at the highest load bins. All the abovementioned observations hold true for all test routes used in this study.

Particle number emissions are shown in Fig. 3. Similar to PM mass and soot mass emissions, particle number emissions exhibited strong, statistically significant decreases with the use of catalyzed GPFs for GDI1 and GDI2 over all test routes. It is worth noting that all vehicles with and without GPFs were below the Euro 6c limit for solid particle number emissions at 6×10^{11} #/km, with the only exception of GDI2 on the Mt. Baldy route. For the Mt. Baldy route, the GPF performance was calculated for the entire trip, which included uphill and downhill driving. For the uphill driving, GDI2 showed an almost negligible particle number reduction (~6%), whereas the particle number reduction for the downhill driving was about 93%. The large discrepancies in the particle number emissions reductions of GDI2 will be discussed later in more detail.

Particle number emissions were seen at higher levels for the urban test routes compared to the Highway route. It is reasonable to assume that the enriched combustion that occurred during frequent stop-and-go events in congested situations resulted in elevated particle number emissions for the urban test routes. The relatively lower particle number emissions for the Highway route could likely be due to the high engine load and high speed, which increased the in-cylinder temperature and improved the mixing of fuel with air, leading to lower particle number emissions. The Downtown SD route also showed some increases in particle number emissions compared to the Downtown LA route, which can be ascribed to some of the unique topological characteristics of the Downtown SD route, such as uphill/downhill driving and a portion of highway driving.

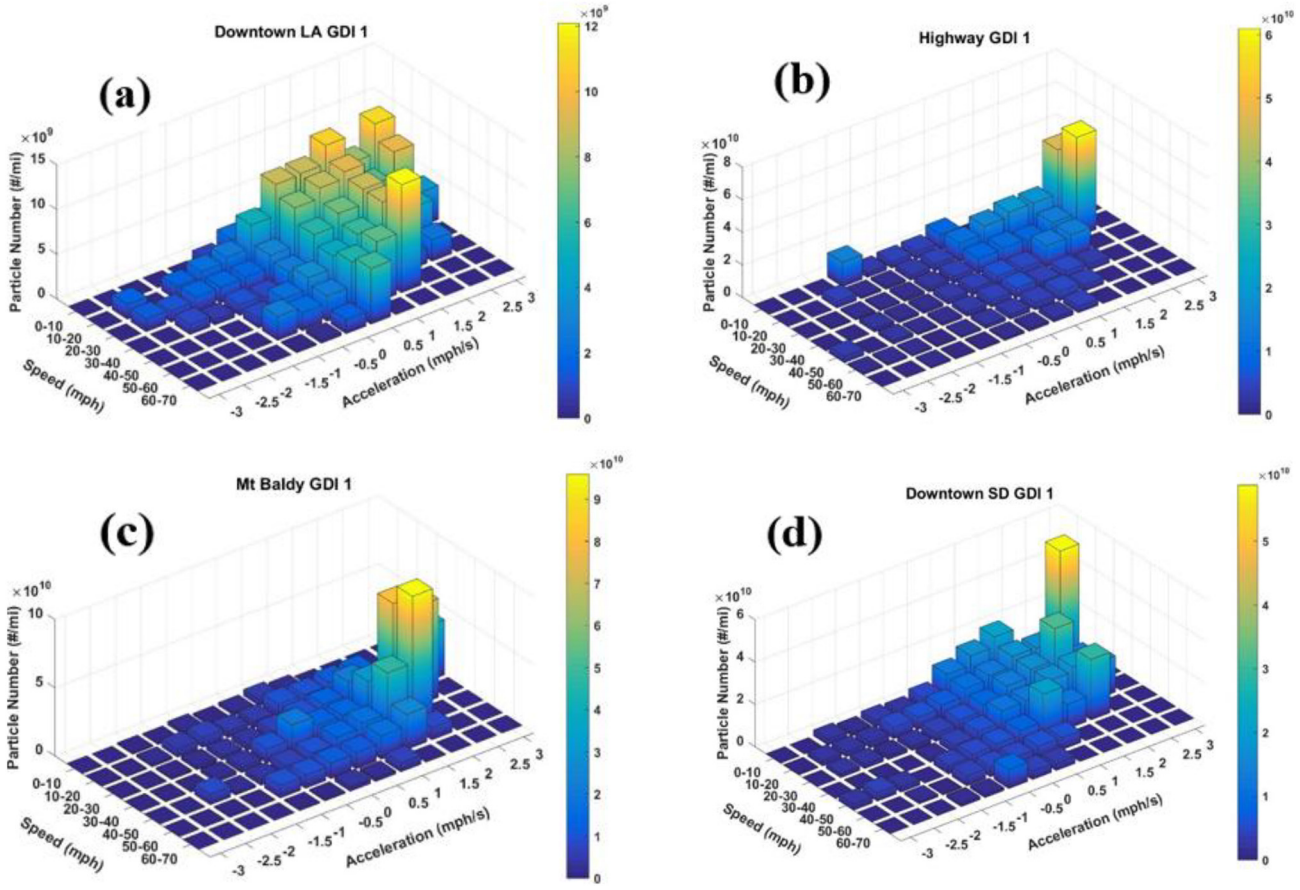

Fig. 2. (a–d): Solid particle number emissions for GDI1 as a function of vehicle speed and acceleration over the Downtown LA (a), Highway (B), Mt. Baldy (c), and Downtown SD (d) test routes.

It is interesting to note the significantly higher particle number emissions for GDI2 over the Mt. Baldy route compared to the other vehicles. The vast majority of particles were produced during the uphill segment of the Mt. Baldy route followed by the urban segment, as shown in Table SM2, SM. As mentioned earlier, particle number measurements for GDI2 were made with the NTK NCEM unit, which uses diffusion charging principle and infers particle number emissions assuming a log-normal particle size distribution with a specific geometric mean diameter, whereas the AVL M.O.V.E PN PEMS iS unit was used for GDI1 and GDI3 to measure solid particle number. It was hypothesized that the higher engine loading when driving over the mountainous roads caused the elevated formation of small volatile or solid particles in the raw exhaust, which agrees with findings from a recent study that showed gasoline vehicles could produce significant concentrations of solid particles below 23 nm (Giechaskiel et al., 2018). Similar phenomena were also observed in an earlier study by Zheng et al. (2014). They reported that aggressive uphill driving led to significant increase in particle emissions above 23 nm for a heavy-duty diesel vehicle with DPF. Since the particle number sensor was direct type to the exhaust and did not have a volatile particle remover (VPR) to remove semivolatile components from the aerosol stream, it counted both volatile and solid particles. For the mountainous route, the phenomena of condensation and nucleation of volatile raw exhaust gas components in the size range below 23 nm downstream of the GPF, were much more prevalent than for the urban and highway test routes for this vehicle, especially during the uphill segment of Mt. Baldy. Therefore, we propose testing on GDI2 did not exactly show a volatile artifact during measurement, but instead a design weakness or oversensitivity of the particle number sensor, which could be resolved by changing the trap voltage in the diffusion charger to include the cut-off of particles below 23 nm. In addition, the poor PM and soot percentage reduction for GDI2 over Mt. Baldy does not suggest poor performance of the catalyzed GPF beyond its function to trap solid soot particles, but it does show the tendency of a catalyzed GPF to store semivolatile particles in the washcoat and release them as secondary nucleated particles under certain types of driving conditions.

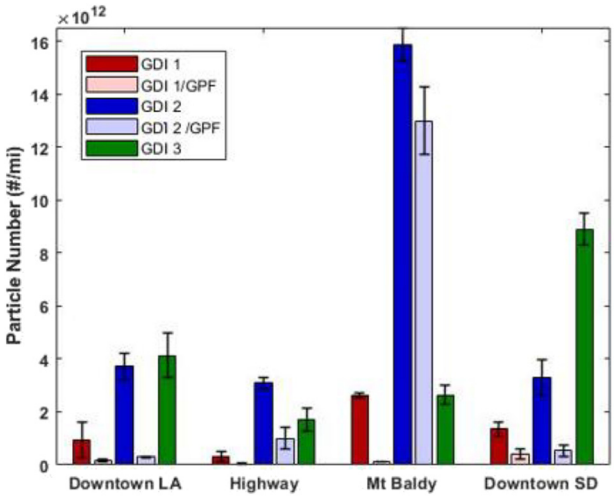

Fig. 3. Particle number emissions for the test vehicles over the different routes.

3.2. Gaseous emissions

NOx emissions for all vehicles and test routes are shown in Fig. 4. NOx emissions in grams per mile ranged from 0.003–0.066 for the Downtown LA route, 0.007–0.035 for the Highway route, 0.013–0.027

for the Mt. Baldy route, and 0.011–0.085 for the Downtown SD route. GDI1 showed 3–4 times higher NOx emissions for all test routes compared to the certification standard for this engine, while GDI2 testing only exceeded the NOx emissions standard over the Highway route. Higher real-world NOx emissions were also seen for GDI3 compared to the certification standard for this engine for all test routes except the Downtown LA route. These are important findings considering that adverse health effects of NO_2 and NOx emissions will affect urban air pollution by participating in the ground level ozone formation. It should be noted that the Los Angeles Basin faces significant air quality issues due to smog concentrations and is currently under EPA's (Environmental Protection Agency) nonattainment designation for ozone.

Results showed a strong dependency between NOx emissions, the different test routes, and the test vehicles, with both urban routes having higher NOx emission levels for GDI1 and lower NOx emission levels for GDI2 and GDI3, respectively, compared to the Highway and Mt. Baldy routes. Overall, GDI1 showed higher NOx emissions than the others vehicles, which was likely due to the relatively higher compression ratio for this vehicle causing increases in the in-cylinder combustion temperature that favored thermal NOx production. Although the primary function of the catalyzed GPF was to eliminate particulate emissions, the additional catalytic surface enhanced the conversion of NOx emissions for both GDI1 and GDI2, provided statistically significant NOx reductions for some test routes. Previous studies have also reported NOx reductions from GDI vehicles with catalyzed GPFs (Yang et al., 2018b; Xia et al., 2017). A different study, however, did not show any further NOx reductions when they tested a GDI vehicle with and without a catalyzed GPF on-road (Demuynck et al., 2017). Table SM2, SM presents the NOx emissions for the four different segments of the Mt. Baldy route (i.e., uphill, downhill, urban, and highway driving). For GDI2 and GDI3, NOx emissions were higher during uphill driving, while urban and highway driving NOx emissions were higher for all vehicles compared to downhill driving. The relatively high NOx emissions for GDI1 over the urban segment and low NOx emissions over the uphill segment could be attributed to the engine combustion strategies associated with this vehicle's driving behavior over different driving conditions (i.e., road grade, start/stop). Our results agree with previous studies that have also shown higher NOx emissions with uphill driving (Gallus et al., 2017; Prati et al., 2015). It was also evident that for the uphill segment of the Mt. Baldy route, lambda (λ) values were closer to stoichiometric and above (lean engine operation), resulting in elevated NOx emissions for all test vehicles. A recent study also reported a strong linkage between real-world NOx emissions and lean engine operation (Suarez-Bertoa et al., 2019).

Comparing the two urban routes, all vehicles showed higher NOx emissions over the Downtown SD route. There may be many contributing factors that could have led to more NOx on the Downtown SD route, including driving conditions and regional variations in temperature and humidity in the area of testing. The increased humidity in the inlet air and its subsequent higher moisture content would have been expected to reduce NOx emissions due to the reduced peak in-cylinder temperature. It appeared that climatic conditions had no effect on NOx emissions, but rather the higher NOx levels for the Downtown SD route were due to the higher engine load during uphill/downhill and highway driving for this route compared to the flat road driving in the Downtown LA route.

CO emissions are shown in Fig. 5. Note that CO emissions were reduced by a factor of 20 for the Mt. Baldy route in Fig. 5 to show comparisons with the other routes. CO emissions were found to be above the certification standards for GDI1 on the Mt. Baldy and Downtown SD routes, GDI2 for the Highway route, and GDI3 for all test routes except Mt. Baldy. Unlike NOx, CO emissions did not show reductions with the catalyzed GPFs over real-world conditions, which contradicts a previous study that showed CO reductions with GPFs over the LA92 cycle (Yang et al., 2018b). CO emissions were found to be higher for the more dynamic Downtown SD route compared to the Downtown LA route, due to more transition engine operating conditions and higher loads that favor rich air-fuel mixtures. Similarly, Demuynck et al. (2017) and Suarez-Bertoa et al. (2019) reported higher real-world CO emissions over more dynamic routes. Results reported here indicate the effects from rich engine operation during uphill/downhill and high-speed driving conditions for the Downtown SD route compared to the flat road Downtown LA route. The Highway route generally showed higher CO emissions compared to both urban routes. For some vehicles, CO emissions were higher over the mountainous roads than the Highway route. Although CO emissions were expected to increase with high altitude and lower atmospheric pressure conditions, this was not the case for some of the vehicles, suggesting that emissions strategies affecting conversion rates in the TWC may have played a role during mountainous driving. However, looking at the uphill segment of the Mt. Baldy route, it is evident that CO emissions were higher compared to the downhill segment (Table SM2, SM). The uphill segment represents typical engine operation with low air-fuel ratios during acceleration events, which favor CO emissions formation.

CO_2 emission rates increased with engine displacement (i.e., GDI3), indicating important CO_2 savings for smaller downsized engines (Fig. SM6, SM). The use of catalyzed GPFs did not show any appreciable CO_2 emission penalties for GDI1 and GDI2. Overall, CO_2 emissions showed an increasing trend for both urban routes, with the Downtown SD route showing higher CO_2 emissions due to higher engine loads for uphill driving relative to flat road driving. For the uphill segment of the Mt. Baldy route, CO_2 emissions were on average 80%–92% higher

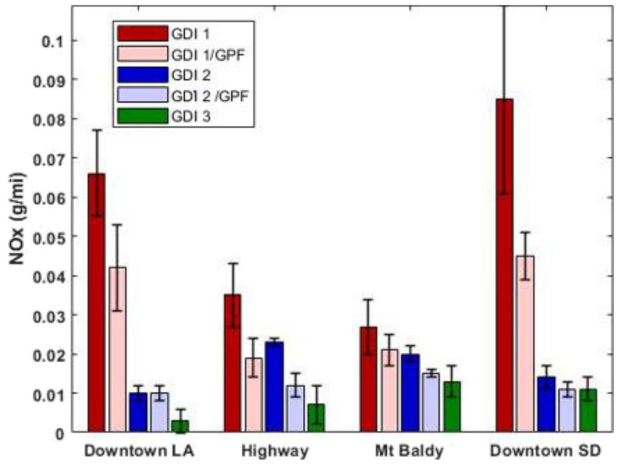

Fig. 4. NOx emissions for the test vehicles over the different routes.

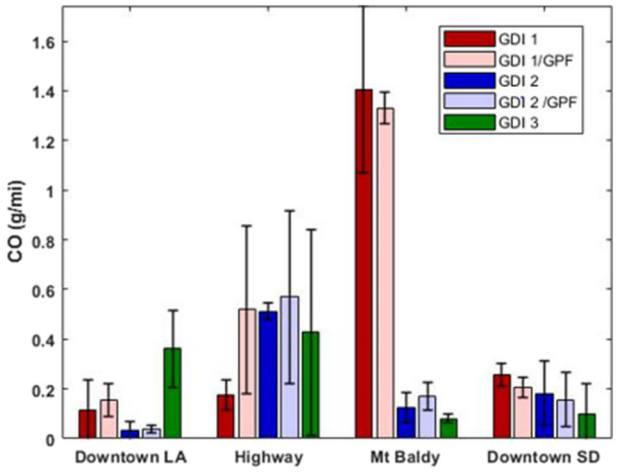

Fig. 5. CO emissions for the test vehicles over the different routes; Note the CO emissions for the Mt. Baldy route are divided by a factor of 20 for all test vehicles.

than during the downhill segment of this route. Similar findings have been reported by Chong et al. (2018), where they showed that higher engine loadings will increase CO_2 emissions due to higher fuel consumption. Wyatt et al. (2013) attributed the higher uphill CO_2 emissions to the increased power demand required to maintain speed or acceleration of the vehicle to overcome the effect of gravity acting as a breaking force that increases with road grade. In addition, the GPF retrofitted vehicles showed higher CO_2 emissions than the original configuration for the uphill segment, with CO_2 increases ranging from 0.9% to 7.8% for GDI1 and GD2, respectively. CO_2 reductions for the downhill segment ranged from 11.7% to 17.2% for GDI1 and GDI2, respectively.

3.3. Cold-start emissions

For the purpose of this analysis, the cold-start increment was defined as the first 5 min after initial start of the engine or until the coolant temperature had reached 70 °C for the first time. Fig. SM7(a–b) (SM) shows the real-time soot mass and particle number emissions evolution for the cold-start period. Both soot mass and particle number populations were significantly higher during the first 50 s of the cold-start period, whereas gradual reductions in both pollutants were seen due to the warm-up of the TWC, engine, and exhaust surfaces. It is noteworthy that the use of GPFs resulted in large reductions of both soot mass and particle number emissions, indicating their beneficial role at the remediation of these pollutants. All vehicles showed different heat-up rates in achieving the coolant warm-up temperature value of 70 °C, with GDI1 and GDI3 reaching full warm-up temperature at 386 s and 266 s, respectively. GDI1 showed the higher particle number and soot mass emissions during the first 50 s and had the lowest coolant temperature and longer heat-up period, followed by GDI3 and GDI2. PM formation during cold-start operation for GDI engines is particularly sensitive, since the injected fuel lands on the cold piston surfaces resulting in the formation of liquid fuel films that fail to completely evaporate, causing diffusive combustion and the formation of soot particles (Chen et al., 2017; Koczak et al., 2016; Yang et al., 2019). Fig. 6(a–d) present the soot mass, particle number, NOx and CO emissions for all vehicles on the Downtown LA route with and without cold-start emissions respectively. For most cases, the inclusion of the cold-start did not show significant differences in soot mass and particle number emissions, with the exception of GDI1. The limited differences between tests could be due to the total distance covered in the test route compared to the short distance and duration of the cold-start period. In addition, the transient and dynamic operation significantly contributes to soot mass and particle number emissions. In agreement with previous studies, CO emissions were significantly affected by the inclusion of cold-start, showing the low conversion efficiency for the TWC when it is below its light-off temperature, while NOx emissions showed lower sensitivity for cold-starts (Merkisz et al., 2019; Khan and Frey, 2018).

4. Conclusions

A reduction in real-world emissions from GDI vehicles is essential for air quality and health in populated areas and megacities. This study investigated on-road gaseous and particle emissions from three current technology GDI vehicles using PEMS. Two vehicles were also retrofitted with catalyzed GPFs to evaluate whether this technology is able to reduce on-road ultrafine particles and black carbon emissions and ultimately improve air quality. Testing was conducted on four test routes

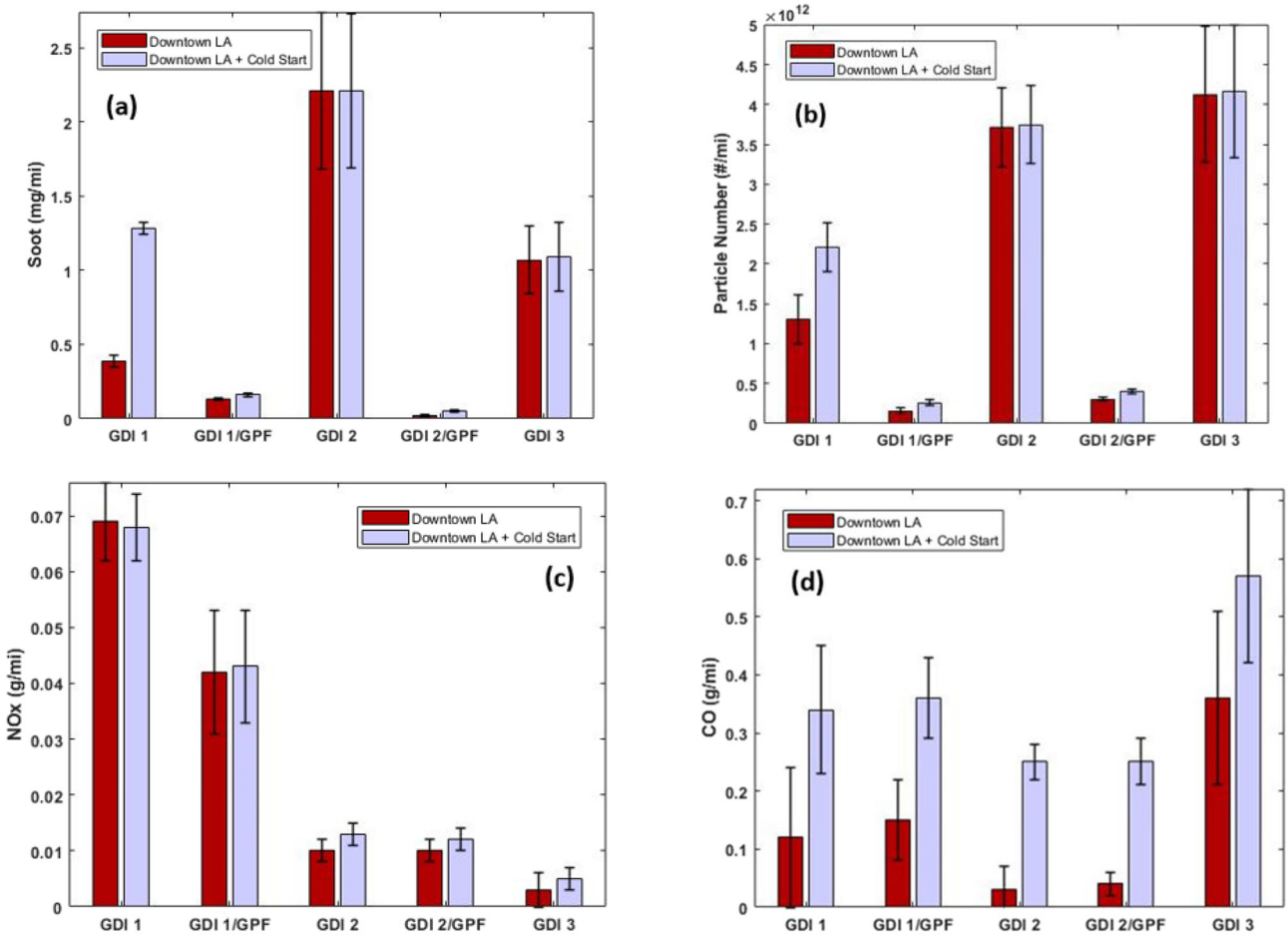

Fig. 6. (a–d): Emissions of soot mass (a), particle number (b), NOx (c), and CO 611 (d) over the Downtown LA route with and without 612 the inclusion of the cold-start phase.

in the greater LA Basin and San Diego representing urban, rural, highway, and high-altitude driving patterns. Results revealed significant reductions in soot mass and solid particle number emissions with the catalyzed GPFs. Mountainous driving showed elevated PM emissions compared to driving without elevation change. The highest PM emissions were seen for the urban routes where public exposure is highest. For all test routes, the highest soot mass and particle number emissions were recorded for the low and intermediate speed bin and high acceleration events. The spread in NOx emissions was lower with the catalyzed GPFs due to the additional catalytic volume compared to the original configuration, suggesting additional NOx reductions in real-driving conditions. Unlike NOx, CO emissions did not show any benefits with the GPFs. Emissions of CO_2 were found to be a function of engine size and were greater for the urban routes, as well as for the uphill segment. The use of GPFs did not show a statistically significant penalty in CO_2 emissions and fuel economy during real-world operation.

Declaration of competing interest

I, Georgios Karavalakis on behalf of the co-authors of this manuscript, certify that we have NO affiliations with or involvement in any organization or entity with any financial interest (such as honoraria; educational grants; participation in speakers' bureaus; membership, employment, consultancies, stock ownership, or other equity interest; and expert testimony or patent-licensing arrangements), or non-financial interest (such as personal or professional relationships, affiliations, knowledge or beliefs) in the subject matter or materials discussed in this manuscript.

Acknowledgements

We acknowledge funding from the South Coast Air Quality Management District (SCAQMD), United States under contract 17331 and the Manufacturers of Emission Controls Association (MECA), United States under contract 15040420. The authors thank MECA for providing the catalyzed GPFs for this program and also for their technical support and guidance.

Appendix A. Supplementary data

Supplementary data to this article can be found online at https://doi.org/10.1016/j.scitotenv.2019.136366.

References

Alkidas, A.C., 2007. Combustion advancements in gasoline engines. Energy Convers. Manag. 48, 2751–2761.
Andersson, J., May, J., Favre, C., Bosteels, D., de Vries, S., Heaney, M., Keenan, M., Mansell, J., 2014. On-road and chassis dynamometer evaluations of emissions from two euro 6 diesel vehicles. SAE Technical Paper (2014-01-2826).
Araji, F., Stokes, J., 2019. Evaluation of Emissions from Light Duty Trucks with and without the Use of a Gasoline Particulate Filter. SAE Technical Paper (2019-01-0971).
Bates, J.T., Weber, R.J., Abrams, J., Verma, V., Fang, T., Klein, M., Tolbert, P.E., 2015. Reactive oxygen species generation linked to sources of atmospheric particulate matter and cardiorespiratory effects. Environ. Sci. Technol. 49, 13605–13612.
Bishop, J.D.K., Molden, N., Boies, A.M., 2019. Using portable emissions measurement systems (PEMS) to derive more accurate estimates of fuel use and nitrogen oxides emissions from modern euro 6 passenger cars under real-world driving conditions. Appl. Energy 242, 942–973.
Cao, T., Durbin, T.D., Russell, R.L., Cocker III, D.R., Scora, G., Maldonado, H., Johnson, K.C., 2016. Evaluations of in-use emission factors from off-road construction equipment. Atmos. Environ. 147, 234–245.
Cao, T., Russell, R.L., Durbin, T.D., Cocker III, D.R., Burnette, A., Calavita, J., Maldonado, H., Johnson, K.C., 2018. Characterization of the emissions impacts of hybrid excavators with a portable emissions measurement system (PEMS)-based methodology. Sci. Total Environ. 635, 112–119.
Chan, T.W., Meloche, E., Kubsh, J., Brezny, R., 2014. Black carbon emissions in gasoline exhaust and a reduction alternative with a gasoline particulate filter. Environ. Sci. Technol. 48, 6027–6034.
Chen, L., Liang, Z., Zhang, X., Shuai, S., 2017. Characterizing particulate matter emissions from GDI and PFI vehicles under transient and cold start conditions. Fuel 189, 131–140.
Chong, H.S., Park, Y., Kwon, S., Hong, Y., 2018. Analysis of real driving gaseous emissions from light-duty diesel vehicles. Transp. Res. Part D: Transp. Environ. 65, 485–499.
Chossière, G.P., Malina, R., Allroggen, F., Eastham, S.D., Speth, R.L., Barrett, S.R.H., 2018. Country- and manufacturer-level attribution of air quality impacts due to excess NOx emissions from diesel passenger vehicles in Europe. Atmos. Environ. 189, 89.
Demuynck, J., Favre, C., Bosteels, D., Hamje, H., Andersson, J., 2017. Real-world emissions measurements of a gasoli e direct injection vehicle without and with a gasoline particulate filter. SAE Technical Paper (2017-01-0985).
Fontaras, G., Zacharof, N.G., Ciuffo, B., 2017. Fuel consumption and CO2 emissions from passenger cars in Europe–laboratory versus real-world emissions. Prog. Energy Combust. Sci. 60, 97–131.
Gallus, J., Kirchner, U., Vogt, R., Borensen, C., Benter, T., 2016. On-road particle number measurements using a portable emission measurement system (PEMS). Atmos. Environ. 124, 37–45.
Gallus, J., Kirchner, U., Vogt, R., Benter, T., 2017. Impact of driving style and road grade on gaseous exhaust emissions of passenger vehicles measured by a portable emission measurement system (PEMS). Transp. Res. D 52, 215–226.
Giechaskiel, B., Lähde, T., Suarez-Bertoa, R., Clairotte, M., Grigoratos, T., Zardini, A., Perujo, A., Martini, G., 2018. Particle number measurements in the European legislation and future JRC activities. Combust. Engine. 174, 3–16.
Huang, C., Lou, D., Hu, Z., Feng, Q., Chen, Y., Chen, C., Tan, P., Yao, D., 2013. A PEMS study of the emissions of gaseous pollutants and ultrafine particles from gasoline- and diesel-fueled vehicles. Atmos. Environ. 77, 703–710.
Johnson, K.C., Durbin, T.D., Cocker III, D.R., Miller, W.J., Bishnu, D.K., Maldonado, H., Moynahan, N., Ensfield, C., Laroo, C.A., 2009. On-road comparison of a portable emission measurement system with a mobile laboratory for a heavy-duty diesel vehicle. Atmos. Environ. 43, 2877–2883.
Kampa, M., Castanas, E., 2008. Human health effects of air pollution. Environ. Pollut. 15, 362–367.
Karavalakis, G., Short, D., Vu, D., Russell, R., Hajbabaei, M., Asa-Awuku, A., Durbin, T.D., 2015. Evaluating the effects of aromatics content in gasoline on gaseous and particulate matter emissions from SI-PFI and SI-DI vehicles. Environ. Sci. Technol. 49, 7021–7031.
Karlsson, R.B., Heywood, J.B., 2001. Piston fuel film observations in an optical access GDI engine. SAE Technical Paper (2001-01-2022).
Khan, T., Frey, H.C., 2018. Comparison of real-world and certification emission rates for light duty gasoline vehicles. Sci. Total Environ. 622–623, 790–800.
Koczak, J., Boehman, A., Brusstar, M., 2016. Particulate emissions in GDI vehicle transients: An examination of FTP, HWFET, and US06 measurements. SAE Technical Paper (2016-01-0992).
Kwon, S., Park, Y., Park, J., Kim, J., Choi, K.H., Cha, J.S., 2017. Characteristics of on-road NOx emissions from euro 6 light-duty diesel vehicles using a portable emissions measurement system. Sci. Total Environ. 576, 70–77.
May, J., Bosteels, D., Favre, C., 2014. An assessment of emissions from light-duty vehicles using PEMS and chassis dynamometer testing. SAE Technical Paper (2014-01-1581).
Mendoza-Villafuerte, P., Suarez-Bertoa, R., Giechaskiel, B., Riccobono, F., Bulgheroni, C., Astorga, C., Perujo, A., 2017. NOx, NH3, N2O, and PN real driving emissions from a euro VI heavy-duty vehicle. Impact of regulatory on-road test conditions on emissions. Sci. Total Environ. 609, 546–555.
Merkisz, J., Bielaczyc, P., Pielecha, J., Woodburn, J., 2019. RDE testing of passenger cars: The effect of the cold start on the emissions results. SAE Technical Paper (2019-01-0747).
O'Driscoll, R., Stettler, M.E.J., Molden, N., Oxley, T., ApSimon, H.M., 2018. Real world CO2 and NOx emissions from 149 euro 5 and 6 diesel, gasoline and hybrid passenger cars. Sci. Total Environ. 621, 282–290.
Ogata, T., Makino, M., Aoki, T., Shimoda, T., Kato, K., Nakatani, T., Nagata, K., Vogt, C.D., Ito, Y., Their, D., 2017. Particle number emission reduction for GDI engines with gasoline particulate filters. SAE Technical Paper (2017-01-2378).
Piock, W., Hoffmann, G., Berndorfer, A., Salemi, P., Fusshoeller, B., 2011. Strategies towards meeting future particulate matter emission requirements in homogeneous gasoline direct injection engines. SAE Int. J. Engines 4, 1455–1468.
Prati, M., Meccariello, G., Della Ragione, L., Costagliola, M., 2015. Real driving emissions of a light-duty vehicle in Naples. Influence of road grade. SAE Technical Paper (2015-01-2509).
Quiros, D.C., Thiruvengadam, A., Pradhan, S., Besch, M., Thiruvengadam, P., Demirgok, B., Carder, D., Oshinuga, A., Huai, T., Hu, S., 2016. Real-world emissions from modern heavy-duty diesel, natural gas, and hybrid diesel trucks operating along major California freight corridors. Emission Control Science and Technology 2, 156–172.
Roth, P., Yang, J., Fofie, E., Cocker III, D.R., Durbin, T.D., Brezny, R., Geller, M., Asa-Awuku, A., Karavalakis, G., 2019. Catalyzed gasoline particulate filters reduce secondary organic aerosol production from gasoline direct injection vehicles. Environ. Sci. Technol. 53, 3037–3047.
Saliba, G., Saleh, R., Zhao, Y., Presto, A.A., Lamber, A.T., Frodin, B., Sardar, S., Maldonado, H., Maddox, C., May, A.A., Drozd, G.T., Goldstein, A.H., Russell, L.M., Hagen, F., Robinson, A.L., 2017. Comparison of gasoline direct-injection (GDI) and port fuel injection (PFI) vehicle emissions: emission certification standards, cold-start, secondary organic aerosol formation potential, and potential climate impacts. Environ. Sci. Technol. 51, 6542–6552.
Schoenhaber, J., Kuehn, N., Bradler, B., Richter, J.M., Bauer, S., Lenzen, B., Beidl, C., 2017. Impact of European real-driving-emission legislation on exhaust gas aftertreatment systems of turbocharged direct injected gasoline vehicles. SAE Technical Paper (2017-01-0924).
Suarez-Bertoa, R., Valverde, V., Clairotte, M., Pavlovic, J., Giechaskiel, B., Franco, V., Kregar, Z., Astorga, C., 2019. On-road emissions of passenger cars beyond the boundary conditions of the real-driving emissions test. Environ. Res. 176, 108572.

Valverde, V., Mora, B.A., Clairotte, M., Pavlovic, J., Suarez-Bertoa, R., Giechaskiel, B., Astorga-LLorens, C., Fontaras, G., 2019. Emission factors derived from 13 euro 6b light-duty vehicles based on laboratory and on-road measurements. Atmosphere 10, 243.

Wang, H., Ge, Y., Hao, L., Xu, X., Tan, J., Li, J., Wu, L., Yang, J., Yang, D., Peng, J., Yang, J., Yang, R., 2018. The real driving emission characteristics of light duty diesel vehicle at various altitudes. Atmos. Environ. 191, 126–131.

Weiss, M., Bonnel, P., Hummel, R., Provenza, A., Manfredi, U., 2011. On-road emissions of light-duty vehicles in Europe. Environ. Sci. Technol. 45, 8575–8581.

Wyatt, D.W., Li, H., Tate, J., 2013. Examining the influence of road grade on vehicle specific power (VSP) and carbon dioxide (CO_2) emission over a real-world driving cycle. SAE Technical Paper (2013-01-1518).

Xia, W., Zheng, Y., He, X., Yang, D., Shao, H., Remias, J., Roos, J., Wang, Y., 2017. Catalyzed gasoline particulate filter (GPF) performance: Effect of driving cycle, fuel, catalyst coating. SAE Technical Paper (2017-01-2366).

Yang, J., Durbin, T.D., Jiang, Y., Tange, T., Karavalakis, G., Cocker III, D.R., Johnson, K.C., 2018a. A comparison of a mini-PEMS and a 1065 compliant PEMS for on-road gaseous and particulate emissions from a light duty diesel truck. Sci. Total Environ. 640–641, 364–376.

Yang, J., Roth, P., Durbin, T.D., Johnson, K.C., Cocker III, D.R., Asa-Awuku, A., Brezny, R., Geller, M., Karavalakis, G., 2018b. Gasoline particulate filters as an effective tool to reduce particulate and PAH emissions from GDI vehicles: a case study with two GDI vehicles. Environ. Sci. Technol. 52, 3275–3284.

Yang, J., Roth, P., Ruehl, C.R., Shafer, M.M., Antkiewicz, D.S., Durbin, T.D., Cocker, D., Asa-Awuku, A., Karavalakis, G., 2019. Physical, chemical, and toxicological characteristics of particulate emissions from current technology gasoline direct injection vehicles. Sci. Total Environ. 650, 1182–1194.

Yoshioka, F., Kato, K., Aoki, T., Makino, M., Waters, D., Jahnke, H., Striebel, F., 2019. Performance of next generation gasoline particulate filter materials under RDE conditions. SAE Technical Paper (2019-01-0980).

Zhang, L., Hu, X., Qiu, R., Lin, J., 2019. Comparison of real-world emissions of LDGVs of different vehicle emission standards on both mountainous and level roads in China. Transp. Res. D 69, 24–39.

Zheng, Z., Durbin, T.D., Xue, J., Johnson, K.C., Li, Y., Hu, S., Huai, T., Ayala, A., Kittelson, D.B., Jung, H.S., 2014. Comparison of particle mass and solid particle number (SPN) emissions from a heavy-duty diesel vehicle under on-road driving conditions and a standard testing cycle. Environ. Sci. Technol. 48, 1779–1786.

Zinola, S., Raux, S., Leblanc, M., 2016. Persistent particle number emissions sources at the tailpipe of combustion engines. SAE Technical Paper (2016-01-2283).

View publication stats